Intra-Node Excess Power Loss Localization Based on Signal Nonlinear Distortion in Optical Fiber Links

Kaixuan Sun(1), Zhenming Yu(1*), Hongyu Huang(1), Xiangyong Dong(1), Kun Xu(1)

(1) State Key Laboratory of Information Photonics and Optical Communications, Beijing University of Posts and Telecommunications, China. Corresponding author: *yuzhenming@bupt.edu.cn.

Abstract *We propose an intra-node excess power loss localization scheme based on receiver DSP using signal nonlinear distortion. Extensive results show that the scheme can successfully locate excess attenuation of WSSs and insufficient amplification of EDFAs of as little as 1 dB.*

Introduction

The traffic carried in optical fiber transmissions is increasing with the rapid expansion of services. The basis for ensuring transmission quality is the stable operation of the optical networks, but the novel flexible architectures that are currently demonstrating potential, such as reconfigurable optical add and drop multiplexer-based optical networks, are failure-prone [1]. If such failures are not dealt with in time, the network will be significantly impacted, which may lead to communication interruptions. Proactive, accurate, and effective failure management is therefore crucial for guaranteeing the quality of service, which several recent studies [2]–[5] have reported. As the key to failure management, it is important to locate the anomalous devices accurately and rapidly for timely follow-up processing.

With the widespread deployment of monitoring equipment, such as optical spectrum analyzers, failures can be localized by detecting changes in the optical spectral shape [6]. However, additional monitoring equipment increases costs, even to the point of unaffordability. Using digital signal processing (DSP) on the receiver side, a reference signal can be analyzed to allow recognition of distance-wise optical power along an end-to-end optical path and thus allow fiber losses to be located [7]. Another method uses artificial neural networks to obtain the power spectrum density of received signals and the tap coefficients of the adaptive filter from the receiver DSP and locates failures related to wavelength selection switches (WSS) based on the interaction between the amplifier spontaneous emission noise and the filtering effect of the WSS [8]. However, none of these schemes involve locating excess power losses in intra-nodes.

In this paper, an intra-node excess power loss localization scheme based on a single receiver DSP and using signal nonlinear distortion is proposed. By compensating to different degrees for the nonlinearity of a received signal and depicting an intensity variance curve along the optical fiber transmission link, the difference between different failure nodes can be clearly identified. We verify the proposed scheme over a four-span, 240-km fiber link with a 30 GBuad polarization division multiplexing (PDM) 16QAM signal transmission. The results show that the scheme can successfully locate excess attenuation of WSSs and insufficient amplification of erbium-doped fiber amplifiers (EDFA) of as little as 1 dB.

Principle

After fiber transmission and coherent detection at the optical link end, standard receiver DSP is employed to process the digitized signal. The proposed intra-node failure localization scheme is based on such a DSP algorithm, as illustrated in Fig. 1. First, linear and nonlinear impairments of the received signal are partially compensated by digital back-propagation (DBP) with a fiber length of $n\Delta l$, where Δl is the resolution of DBP and n=0, 1, 2, …, N is the n-th step. DBP is performed by alternating nonlinear compensation and chromatic dispersion compensation according to a fixed step size. After the partial DBP compensation, the residual chromatic dispersion (CD)—that is, the difference between the total CD and the compensated CD—is compensated. The output signal is then fed into an adaptive equalizer (AEQ), which is demultiplexed using a cascaded multi-modulus algorithm (CMMA) [9]. Next, the intensity variance of the equalizer output $E(t)$ is calculated, which is defined in Eq. (1):

$$\textit{intensity variance} = \sigma^2[|E(t)|^2]. \qquad (1)$$

With increasing n, the degree to which the received signal is compensated gradually increases. Therefore, the value of the intensity variance also increases regularly with the transmission distance.

To locate a failure, a set of intensity variances (IV_{normal}) is first calculated and stored based on all possible n for the entire link under normal

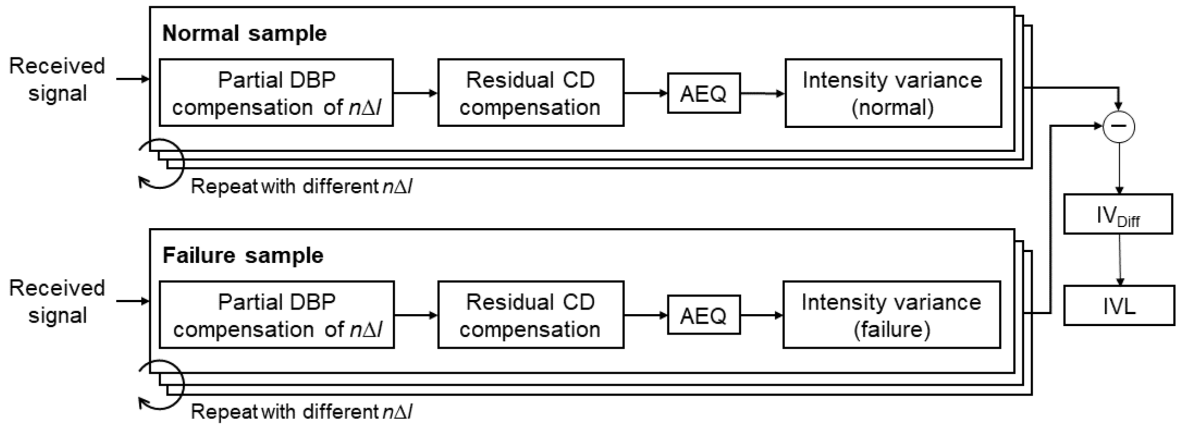

Fig. 1: Framework of the proposed intra-node failure localization scheme. DBP: digital back-propagation, CD: chromatic dispersion, AEQ: adaptive equalizer; IV_{Diff}: difference between the intensity variances of the normal and failure samples; IVL: intensity variance locator.

conditions. When a failure is detected, a set of intensity variances ($IV_{failure}$) is then calculated using the received signal at that time. The failure location can then be determined based on the difference between IV_{normal} and $IV_{failure}$, as expressed in Eq. (2):

$$IV_{Diff} = IV_{normal} - IV_{failure}. \quad (2)$$

The reason is that, in a normal link state, the evolution of the power of a signal that has experienced different transmission distances follows a certain rule. However, when a link suffers from unexpected intermediate loss, such as extra attenuation of WSS, that rule of the evolution of the signal power changes, resulting in a set of intensity variances that differs from the normal state. Moreover, this kind of difference occurs at the failure location, so the failure can be localized. To demonstrate the failure location more visually, we further calculate an intensity variance locator (IVL) based on IV_{Diff}, as expressed in Eq. (3):

$$IVL = IV_{Diff}^{\,t} - IV_{Diff}^{\,t-1}, \quad (3)$$

where t=1, 2, 3, …, T is the t-th component of IV_{Diff}. The failure location can then be clearly determined from the peak of the IVL.

Simulation Setup

A single-channel simulation link was constructed to demonstrate the proposed scheme, as shown in Fig. 2, consisting of four 60-km spans of standard single-mode fiber (SSMF) (attenuation coefficient α=0.2 dB/km, nonlinear coefficient γ=1.3 (W.km)$^{-1}$, dispersion coefficient D=16 ps/nm/km). At the transmitter side, a 30-GBaud PDM 16QAM signal is transmitted with a central wavelength of 1550 nm. The signal is Nyquist-shaped, with a roll-off factor of 0.05, which means a 31.5-GHz optical signal bandwidth. In the normal link state, the fiber launch power into each span is 6 dBm. At the receiver side, the signal is post-amplified, detected, and fed into the off-line DSP. To compensate for nonlinearity, DBP is performed with a step size of 10 km. Thus, each IV_{normal} or $IV_{failure}$ has 25 components corresponding to a curve with a 10-km resolution.

The straight fiber line includes three nodes and four spans of 60 km, without any in-line optical dispersion compensation. Each node has a WSS of 37.5 GHz and an EDFA that compensates for fiber span losses, with a gain of 12 dB in the normal link state. A variable optical attenuator (VOA) adjacent to each WSS is used to introduce WSS-related failure. The proposed scheme is verified with data obtained by artificially introducing the following failures into the setup:

- Excess attenuation of the WSS: introduced by setting the attenuation values of the VOAs at different nodes.
- Insufficient amplification of the EDFA: introduced by the EDFAs at different nodes and

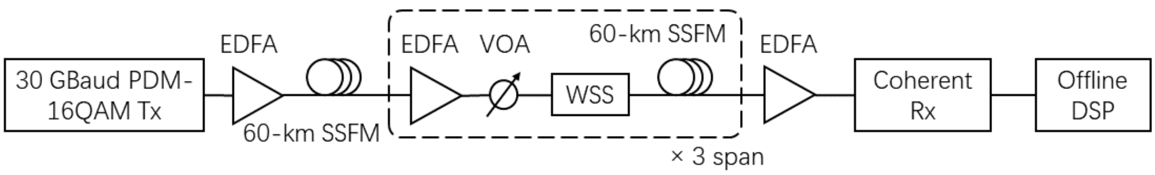

Fig. 2: Simulation setup. Tx: transmitter, EDFA: erbium-doped fiber amplifier, SSMF: standard single-mode fiber, VOA: variable optical attenuator, WSS: wavelength selection switch, Rx: receiver, DSP: digital signal processing.

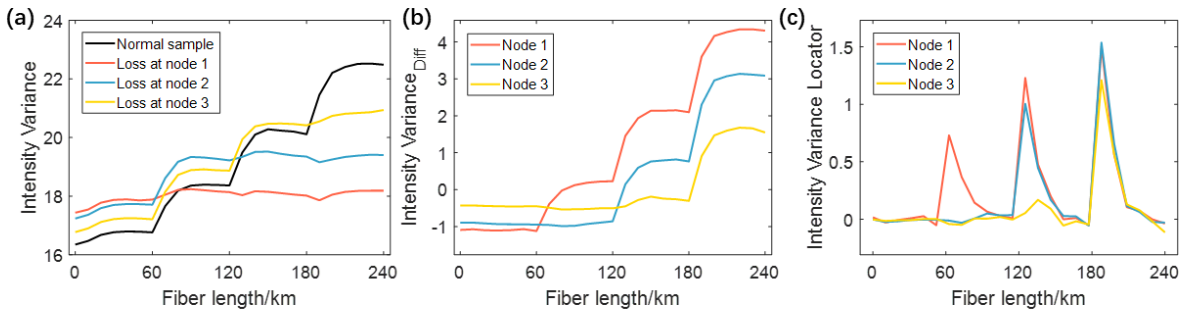

Fig. 3: Localization of the excess attenuations of WSSs at different nodes. (a) intensity variance curves; (b) differences between intensity variances for the normal and failure samples; (c) intensity variance locator curves.

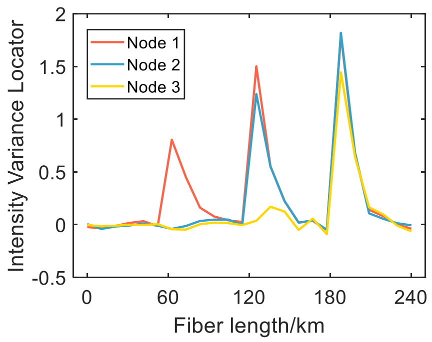

Fig. 4: Intensity variance locator curves for several insufficient EDFA amplifications.

providing insufficient gain for the signals. Note that, when a failure-related parameter is introduced, the other parameters remain unchanged.

Results and Discussion

A normal sample and failure samples at different nodes were collected for analysis. We first investigated the localization of the nodes at which excess attenuation occurred at the WSSs and plotted the curves based on Eq. (1) – Eq. (3), as shown in Fig. 3. The nodes were located at 60 km, 120 km, and 180 km. Fig. 3(a) illustrates how the intensity variance curve of the normal sample shows similar and regular increases in each span. However, when a failure occurs, the trend of the curve, starting from the failure node, is no longer similar to that of the normal sample. In Fig. 3(b), the IV_{Diff} curves for the failure samples and the normal sample are shown. After the failure node, the curve goes up significantly. This difference is more evident in Fig. 3(c). Starting from the failure node, regular peaks appear. The samples that failed at the 1st, 2nd, and 3rd nodes show 3, 2, and 1 peaks in the IVL curves, respectively.

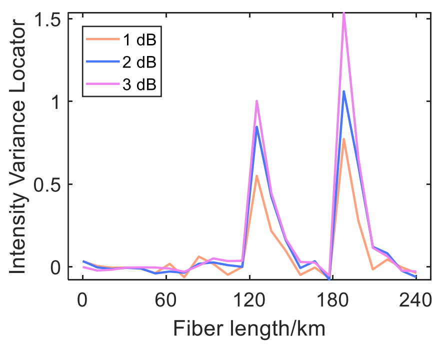

Fig. 5: Intensity variance locator curves for several excess WSS attenuations.

We then tested the failure localization of the insufficient amplification of the EDFAs. The IVL curves are shown in Fig. 4. Similar to the excess attenuation of the WSSs, the insufficient amplification of the EDFAs at the 1st, 2nd, and 3rd nodes are reflected by different peaks, which also means that this kind of failure can be accurately located.

Finally, we investigated the IVL curves with different excess attenuation of the WSSs, as shown in Fig. 5. Failures were introduced at the 2nd node. The results show that the peak value of the IVL curve increases with increased attenuation and that a power loss as little as 1 dB can be successfully located.

Conclusions

We proposed and demonstrated an intra-node excess power loss localization scheme based on the receiver DSP and using signal nonlinear distortion. The difference between the failures of different nodes is determined by calculating the intensity variance with different degrees of nonlinear compensation of the received signal. Our scheme successfully located the excess attenuation of WSSs and insufficient amplification of EDFAs on a 240-km four-span SSMF link transmitting 30 GBaud PDM-16QAM signals.

Acknowledgements

This work was financially supported by the National Key R&D Program of China (No. 2021YFF0901700); the National Natural Science Foundation of China (No. 61821001, 61901045); and the Fund of State Key Laboratory of Information Photonics and Optical Communications, BUPT (No. IPOC2021ZT18).

References

[1] C. Delezoide, K. Christodoulopoulos, A. Kretsis, N. Argyris, G. Kanakis, A. Sgambelluri, N. Sambo, P. Giardina, G. Bernini, D. Roccato, A. Percelsi, R. Morro, H. Avramopoulos, E. Varvarigos, P. Castoldi, P. Layec, and S. Bigo, “Marginless operation of optical networks,” *Journal of Lightwave Technology*, vol. 37, no. 7, pp. 1698–1705, 2019, DOI: 10.1109/JLT.2018.2881840.

[2] F. Musumeci, V. G. Venkata, Y. Hirota, Y. Awaji, S. Xu, M. Shiraiwa, B. Mukherjee, and M. Tornatore, “Domain adaptation and transfer learning for failure detection and failure-cause identification in optical networks across different lightpaths [Invited],” *Journal of Optical Communications and Networking*, vol. 14, no. 2, p. A91, 2022, DOI: 10.1364/JOCN.438269.

[3] K. Sun, Z. Yu, L. Shu, Z. Wan, H. Huang, Y. Lei, and K. Xu, “Digital residual spectrum-based generalized soft failure detection and identification in optical networks,” *IEEE Transactions on Communications*, vol. 71, no. 1, pp. 324–338, 2023, DOI: 10.1109/TCOMM.2022.3222519.

[4] H. Lun, M. Fu, Y. Zhang, H. Jiang, L. Yi, W. Hu, and Q. Zhuge, “A GAN based soft failure detection and identification framework for long-haul coherent optical communication systems,” *Journal of Lightwave Technology*, vol. 41, no. 8, pp. 2312–2322, 2023, DOI: 10.1109/JLT.2022.3227719.

[5] Z. Jiang, X. Tang, S. Wang, G. Gao, D. Jin, J. Wang, and M. Si, “DSP enabled, amplitude modulation pilot tone based optical performance monitoring in coherent systems,” in *2021 European Conference on Optical Communication (ECOC)*, Bordeaux, France: IEEE, 2021, pp. 1–4. DOI: 10.1109/ECOC52684.2021.9605847.

[6] B. Shariati, M. Ruiz, J. Comellas, and L. Velasco, “Learning from the optical spectrum: failure detection and identification,” *Journal of Lightwave Technology*, vol. 37, no. 2, pp. 433–440, 2019, DOI: 10.1109/JLT.2018.2859199.

[7] T. Tanimura, S. Yoshida, K. Tajima, S. Oda, and T. Hoshida, “Fiber-longitudinal anomaly position identification over multi-span transmission link out of receiver-end signals,” *Journal of Lightwave Technology*, vol. 38, no. 9, pp. 2726–2733, 2020, DOI: 10.1109/JLT.2020.2984270.

[8] H. Lun, Y. Wu, M. Cai, X. Liu, R. Gao, M. Fu, L. Yi, W. Hu, and Q. Zhuge, “ROADM-induced anomaly localization and evaluation for optical links based on receiver DSP and ML,” *Journal of Lightwave Technology*, vol. 39, no. 9, pp. 2696–2703, 2021, DOI: 10.1109/JLT.2021.3055850.

[9] X. Zhou, J. Yu, and P. Magill, “Cascaded two-modulus algorithm for blind polarization de-multiplexing of 114-Gb/s PDM-8-QAM optical signals,” in *Optical Fiber Communication Conference and National Fiber Optic Engineers Conference*, San Diego, California: OSA, 2009, p. OWG3. DOI: 10.1364/OFC.2009.OWG3.